Performance of Real-time Precise Point Positioning in New Zealand

Ken HARIMA, Suelynn CHOY and Chris RIZOS, Australia
Kogure SATOSHI, Japan

Key words: GPS, GNSS, PPP, Real-Time

SUMMARY

Most of the GNSS based high accuracy positioning services available today are based on differential techniques like RTK. These kinds of services are only available inside a network of Continuously Operating Reference Stations (CORS) or a few kilometers from such stations. An emerging alternative to these infrastructure heavy method is the Precise Point Positioning (PPP) technique. PPP as a technique aims at delivering centimeter level accuracy positioning without the need of directly connecting to a local CORS. Although PPP still needs to monitor GNSS satellites and compute corrections for their signals, these corrections are calculated computed from sparse global networks. Recent research and development has investigated into satellite broadcast of corrections for PPP. The combination of sparse CORS and satellite delivery make PPP based positioning ideal for situations where local infrastructure is unavailable or unreliable.

The present document studies the potential performance of PPP in New Zealand. PPP is now a quite mature research topic and a number of real-time corrections for PPP are publicly available for testing. Three of these streams are used to calculate real-time kinematic PPP solutions in Auckland, Hastings, Wellington, Yaldhurst (Christchurch), Dunedin and Chatham Island. The selected real-time streams have been tested or are likely to be available as, satellite delivery services. MADOCA messages produced by the Japanese Aerospace Exploration Agency have been in tests using the Quasi-Zenith Satellite System since 2013. CLK81 messages streamed from the IGS real-time server are computed by satellite operators GMV using their MagicGNSS software. Finally the CLK9B message calculated by the French Space Agency (CNES) was broadcast by the QZSS in tests performed in 2014 and 2015.

Results of real-time positioning tests show that accuracies of 6 cm in horizontal positioning and 15 cm in vertical positioning can be achieved by kinematic PPP. The convergence times to 10 cm of horizontal accuracy is about 30 minutes.

Performance of Real-time Precise Point Positioning in New Zealand

Ken HARIMA, Suelynn CHOY and Chris RIZOS, Australia
Kogure SATOSHI, Japan

1. INTRODUCTION

Global Navigation Satellite Systems (GNSS) Precise Point Positioning (PPP) technique has been an active research topic for nearly 20 years. This mode of positioning conforms to the original intention of Global Positioning System (GPS) or GNSS usage, that is, position resolution with a single receiver independent of location or available local infrastructure. Most of the currently established high accuracy positioning services are based on differential positioning techniques like Real-Time Kinematic (RTK). These services account for systematic biases by comparing the observations on the user receiver with those obtained in a nearby reference station. Services like RTK are only available inside a network of Continuously Operating Reference Stations (CORS) or a few kilometers from such stations.

PPP on the other hand, uses a robust modelling of GNSS errors and precise information on satellite orbits, satellite clocks and signal biases to make accurate estimates of the user position (Kouba, 2009; Zumberge et al., 1997). Unlike differential approaches PPP only makes use of information that is valid globally or over wide areas, and thus only requires a sparse network of monitoring stations. Post-processed positioning services based on PPP are now mature and are available from multiple online sources, offering accuracies of 2-3 cm (Grinter & Jansen, 2012). More recent studies are focused on real-time delivery of PPP services and ambiguity resolution for PPP (Ge et al., 2007, Laurichesse et. al 2009). A public Real-Time Service (RTS) to support real-time high precision GNSS applications allows the testing of real-time PPP (IGS, 2015).

The caveats of real-time PPP are the availability of low latency precise satellite orbit and clock information, and communication channels used to disseminate this information. From a practical viewpoint satellite-based broadcasting is an ideal communication link for PPP enabling the strategic advantage of PPP, namely its wide coverage area. A combination of PPP based position and satellite based delivery will be completely independent of local infrastructure, making it ideal for cases where local infrastructure is either unavailable or unreliable. This includes oceans, remote areas but also can be conceived in the aftermath of natural disasters.

In this study, an analysis of the quality of the satellite orbit and clock corrections available from real time stream is presented along with an evaluation of the performance of PPP algorithms using these real-time streams. Three real-time streams were selected for the study, all of them publicly available and all of them tested with satellite transmission. The MDC1 stream is generated by the Japan Aerospace Exploration Agency (JAXA) using the Multi-GNSS Advanced Demonstration tool for Orbit and Clock Analysis (MADOCA) software (JAXA, 2014). The CLK81 stream is generated by GMV using the MagicGNSS software and broadcasted using IGS real-time services. The CLK9B

stream is generated by the French Space Agency (CNES) as part of their PPP-Wizard project. The selected real-time streams have been tested or are likely to be available as satellite delivered services. MADOCA messages produced by the Japanese Aerospace Exploration Agency have been broadcasted by the Quasi-Zenith Satellite System (QZSS) since 2013. CLK81 messages streamed from the IGS real-time server are produced by satellite operators GMV. Finally CLK9B produced by the French Space Agency (CNES) was broadcast by the QZSS in tests performed in 2014 and 2015 (Harima et. al., 2015)

For this study, orbit and clock corrections taken from the real-time streams are combined with observations from CORS in New Zealand to generate PPP solutions. Dual-frequency observables corresponding to signals from GPS and GLONASS satellites are used to calculate the PPP solutions. The solutions are calculated using the RTKLIB software (Takasu and Yasuda, 2009), an open source software for high accuracy positioning.

This paper is structured in five sections. A brief description of the PPP algorithm is given in Section 2. An evaluation of the accuracy of real-time streams available for PPP is presented in Section 3. The performance of real-time PPP using the real time streams is studied in Section 4. A summary of the findings is given in Section 5.

2. PRECISE POINT POSITIONING

In differential approaches (like RTK) errors on the GNSS observations are mitigated by differencing with measurements taken in a nearby station and used directly to correct for errors in measurements at the user receiver. In PPP by contrast, errors are modeled as a combination of errors with different origins. This allows the separation of GNSS errors between those with global validity, like satellite clock and orbit errors, and local errors such as atmospheric effects and receiver biases. Global errors can be estimated using a sparse network and sent to the user for correction. Local errors are either estimated along with the receiver position or compensated by means of linear combinations.

Numerous versions of this core concept have been developed over the past years. This section describes the PPP algorithms used to calculate the positioning solutions presented in section 4. These algorithms, implemented in the RTKLIB software, are based on (Zumberge et al, 1997) for standard PPP and (Ge et al, 2007) for ambiguity resolved PPP.

2.1 Standard PPP algorithm

Standard PPP algorithms use ionosphere-free (IF) linear combinations of measurements from two different carrier frequencies to eliminate the effects of the ionospheric delay, which is the largest error with local variability:

$$P_{IF}^{s} = \rho^{s} + dt - dt^{s} + c_1(B_{P1} - B_{P1}^{s}) + c_2(B_{P2} - B_{P2}^{s}) \quad (1)$$

$$L_{IF}^{s} = \rho^{s} + dt - dt^{s} + c_1(\lambda_1 N_{L1}^{s} + B_{L1} - B_{L1}^{s}) + c_2(\lambda_2 N_{L2}^{s} + B_{L2} - B_{L2}^{s}) \quad (2)$$

where P_{IF}^s is the ionosphere-free combination of P_1 and P_2 code measurements, L_{IF}^s is the ionosphere-free combination of the L_1 and L_2 carrier measurements corrected for antenna phase offsets and phase windup effects. c_1 and c_2 are the ionosphere free linear combination coefficients, λ_1 and λ_2 the wavelength of L_1 and L_2 carriers. ρ^s is a range estimate, which includes the satellite-receiver range and tropospheric delays, dt and dt^s are the receiver and satellite clock offsets. B_{P1} and B_{P1}^s are the receiver and satellite bias for the P_1 code measurement, B_{P2} and B_{P2}^s are the biases for P_2. B_{L1} and B_{L1}^s are the biases for L_1 phase measurements, B_{L2} and B_{L2}^s are the biases for L_2. N_{L1}^s and N_{L2}^s are the integer ambiguities.

For standard PPP, the required global information are the precise satellite orbits, which are used to associate ρ^s with the receiver position, and the ionosphere-free clocks

$$dt_{IF}^s = dt^s + c_1 B_{P1}^s + c_2 B_{P2}^s. \quad (3)$$

Ionosphere-free linear combinations of code and carrier measurements corrected for the ionosphere-free satellite clock, antenna phase offsets and phase windup effects, are used to estimate the receiver position, the zenith tropospheric delay, the receiver ionosphere-free clock, and a "float ambiguity" from the modified measurement model

$$B_{FLT}^s = c_1(\lambda_1 N_{L1}^s + B_{L1} - B_{L1}^s - B_{P1} + B_{P1}^s) + c_2(\lambda_2 N_{L2}^s + B_{L2} - B_{L2}^s - B_{P2} + B_{P2}^s) \quad (4)$$

$$P_{IF}^s + dt_{IF}^s = \rho^s + dt_{IF} \quad (5)$$

$$L_{IF}^s + dt_{IF}^s = \rho^s + dt_{IF} + B_{FLT}^s \quad (6)$$

An extended Kalman Filter is used to estimate the parameters from the measurements. The receiver clock is modelled as a white noise process with the results of a standard, code based solution as the mean. The zenith tropospheric delay is modelled as a random walk process. The "float biases" are modelled as a constant value but monitored for cycle slips using geometry-free carrier phase measurements. Finally the receiver position is modelled as a white noise process with the results of standard code based positioning as the mean.

2.2 Ambiguity resolution in PPP

While consolidating the integer ambiguities and hardware biases into one "floating ambiguity" allows the resolution of position without the transmission of satellite signal biases. Most of the recently proposed PPP algorithms suggest the transmission of these individual biases to attempt integer ambiguity resolution. Ambiguity resolution takes advantage of the fact that the phase ambiguities N_i are integer valued. By solving and fixing the values of N_i to integer values, error associated with these parameters can be eliminated. This in theory will allow the PPP solutions to approach RTK in accuracy.

Several strategies have been proposed for ambiguity resolution in PPP. The method used in the

present study is based on (Ge et al, 2007):

- Measurements are corrected for signal biases
- The standard PPP solution is calculated using corrected measurements.
- The Melbourne-Wübenna combination
  $P_{MW}^{S} = \frac{\lambda_2}{\lambda_2-\lambda_1}L_1^S - \frac{\lambda_1}{\lambda_2-\lambda_1}L_2^S - \frac{\lambda_2}{\lambda_2+\lambda_1}P_1^S - \frac{\lambda_1}{\lambda_2+\lambda_1}P_2^S$ (7)
  is used to separate integer ambiguities from other elements in B_{FLT}^{S}.
- The integer ambiguities are resolved and used to calculate a corrected value for B_{FLT}^{S}.
- The corrected value for B_{FLT}^{S} is used as a measurement to correct the PPP solution.

The single-differenced Melbourne-Wübenna combination of L_1 and L_2 signals, corrected for satellite biases, can be expressed as:

$$P_{MW}^{S} - P_{MW}^{r} = \frac{\lambda_1\lambda_2}{\lambda_2-\lambda_1}(N_{L1}^{S} - N_{L2}^{S} - N_{L1}^{r} + N_{L2}^{r}), \quad (8)$$

here the superscript *r* represents the reference satellite. This Melbourne-Wübenna combination can be used to solve the integer ambiguity combination $N_{L1}^{S} - N_{L2}^{S} - N_{L1}^{r} + N_{L2}^{r}$. Once the ambiguity combination is solved, the single-differenced N_{L1}^{S} ambiguity can be isolated from B_{FLT}^{S}, corrected for satellite biases.

$$B_{FLT}^{S} - B_{FLT}^{r} - c_2\lambda_2[\![N_{L1}^{S} - N_{L2}^{S} - N_{L1}^{r} + N_{L2}^{r}]\!] = \frac{\lambda_1\lambda_2}{\lambda_2+\lambda_1}(N_{L1}^{S} - N_{L1}^{r}) \quad (9)$$

here $[\![N_X^S]\!]$ is used to express the resolved version of the ambiguity N_X^S. Once the ambiguities are resolved, a corrected single differenced value of B_{FLT}^{S}

$$B_{FIX}^{S} - B_{FIX}^{r} = \frac{\lambda_1\lambda_2}{\lambda_2+\lambda_1}[\![N_{L1}^{S} - N_{L1}^{r}]\!] + \lambda_2[\![N_{L1}^{S} - N_{L2}^{S} - N_{L1}^{r} + N_{L2}^{r}]\!] \quad (10)$$

is calculated and used as a measurement to complement the equations (5) and (6) to calculate a corrected position. The ambiguity differences $N_{L1}^{S} - N_{L2}^{S}$are resolved to integer values using the integer rounding method. The N_{L1}^{S}ambiguity is resolved using the modified LAMBDA method (Chang et al, 2009).

2.3 Correction messages for PPP

As explained in previous sections, standard PPP solutions give information on precise satellite orbits and ionosphere-free satellite clocks. Ambiguity resolved PPP additionally require hardware bias estimates for the code and carrier of the GNSS signals. While numerous real-time streams that transmit orbits and clock for GPS exist, streams containing multi-GNSS are still few. GLONASS is still experimental for IGS-RT streams.

Also for real-time processing, the information for PPP needs to be available with a low latency, as these values changes over time. The available real-time streams follow a protocol established by the Radio Technical Commission for Maritime Services (RTCM, 2013). These messages contain corrections to orbit and clock information broadcast by the GNSS satellites. This allows savings in

the transmission bandwidth while still allowing the user to compute precise orbit and clocks. Table 1 shows the update rates of the different types of corrections transmitted by the different real-time streams.

	Orbit	Clock	Other
MDC1	30 sec	1 sec	URA: 1 sec
CLK81	5 sec	5 sec	
CLK9B	5 sec	5 sec	GPS Biases: 5 sec

Table 1. Contents of Real-time messages for PPP

The MDC1 stream updates clock corrections every second, and orbits every 30 seconds, in addition it transmits an estimate of the user range accuracy (URA) each second. The other streams updates orbit and clocks every 5 seconds. At the time of writing, the only publicly available stream known to the authors that transmits signal biases for real-time PPP are streams from CNES PPP-wizard project.

3. REAL TIME STREAMS FOR PPP

The quality of the precise orbits and clock corrections included in the augmentation messages has a direct impact on the achievable accuracy and convergence time of the PPP solutions. In this section we discuss the quality of the orbit and clock corrections included in the real-time streams. Orbits and clock calculated using data from the real-time stream were compared with post-processed versions of the same parameters. The post process solutions used as a reference the IGS rapid products for GPS and IGS final products for GLONASS, these products have an estimated accuracy of 3 cm for orbits and 75ps RMS and 25ps STD (equivalent to 2.25cm and 0.75cm respectively) for clocks (IGS, 2014).

Table 2 summarises the estimated quality of real-time corrections as compared to IGS products. Values in the table are daily standard deviations of range differences for different positions on earth. The range difference, Signal in Space Range Errors (SISRE), can be calculated as follows:

$$SISRE = \left\| \overrightarrow{X_{sat}^{RT}} - \overrightarrow{X_{sta}} \right\| - \left\| \overrightarrow{X_{sat}^{ref}} - \overrightarrow{X_{sta}} \right\| - dt^{RT} + dt^{ref} \qquad (11)$$

SISRE represent the effect of orbit and clock errors will have in the measurement equations (5) and (6).

	Tokyo	Bern	Sydney	Auckland	Chath. Is.	Dunedin
GPS SISRE for MDC1	5.03 cm	6.04 cm	4.90 cm	4.81 cm	4.77 cm	4.77 cm
GPS SISRE for CLK81	16.66 cm	19.50 cm	13.52 cm	16.42 cm	17.20 cm	15.57 cm
GPS SISRE for CLK9B	2.76 cm	9.41cm	2.93 cm	3.05 cm	2.95 cm	3.02 cm
GLO SISRE for MDC1	8.81 cm	10.59 cm	14.28 cm	14.36 cm	15.16 cm	15.61 cm
GLO SISRE for CLK81	8.85 cm	10.92 cm	10.20 cm	9.32 cm	10.01 cm	10.16 cm
GLO SISRE for CLK9B	8.43 cm	10.33 cm	9.04 cm	7.90 cm	9.11 cm	9.73 cm

Table 2. Signal in Space Range Errors in Tokyo, Bern, Sydney and New Zealand.

Also as it will be shown in following subsections, a significant part of the differences between the real-time and reference products were large biases in the clock corrections. These biases were between 10 and 30 cm for GPS and between 50cm and 1m for GLONASS, and constant throughout the day.

These biases, while potentially affecting the convergence time of solutions are not expected to have significant impact on positioning solutions in the steady state. On one hand, a clock bias that is constant over the day (or one satellite pass) will be absorbed in equation (6) by the "float ambiguity" B^s_{FLT}. On the other hand the error levels on the code measurement in equation 5 are in the order of meters. For this reason, a daily Standard deviation (STD) is used in place of RMS as a measure of the quality of real-time orbit and clock corrections.

With a few exceptions mostly attributable to errors in products for the G26 satellite, SISRE values are below 5 cm for GPS and below 11 cm for GLONASS. Also with the exception of MDC1 products for GLONASS, the SISRE have similar values around the world. The product statistics on this section are based on real-time products transmitted on the 30th of September 2015.

3.1 MADOCA from JAXA (MDC1)

Table 3 show the RMS and daily standard deviation errors for the MADOCA generated products. The orbits are expressed in satellite centric RAC coordinates. In this coordinate system the Radial direction is approximately the direction to the center of the earth, the Along-track direction is the direction of the satellite velocity, and the cross track direction is perpendicular to the other two. The

error components with the most influence in the SISRE, and consequently to positioning accuracy, are the radial component and the clock.

The orbits generated by MADOCA products have relatively large differences with respect to the IGS post process orbits. This is to be expected to some extent as the MADOCA orbits are generated independently from the IGS. This is in contrast to the CLK9B stream which uses IGS ultra-rapid orbits and clocks as a base for their orbits.

	Radial	**Along**	**Cross**	**Clock**
RMS GPS	4.83 cm	19.22 cm	14.08 cm	28.76 cm
RMS GLO	5.09 cm	13.87 cm	8.42 cm	50.14 cm
STD GPS	3.08 cm	6.49 cm	10.35 cm	4.81 cm
STD GLO	3.28 cm	7.76 cm	5.06 cm	9.47 cm

Table 3. Errors of MADOCA satellite orbits and clock estimates, 30th of September 2015.

The GPS clocks were found to be as close if not closer than other solutions to the post process IGS clocks. For GPS, the resultant SISRE is similar to the one obtained using the GMV (once the effects of satellite G26 are discarded.

Figure 1 shows the RMS values of orbit errors, radial errors are shown in blue, along-track errors are shown in green, cross-track errors are shown in brown. There are satellites with large along-track and cross-track errors, i.e. G13, G14, G15 and G22. The SISRE values corresponding to those satellites are not significant for test points in Sydney or New Zealand. However they do lead to relatively large SISRE errors in Tokyo and Bern. In particular, the SISRE error for satellite G13 on Bern was about 24.8 cm. However these errors are not expected to lead to significant performance degradation in PPP solutions.

As a last note, the relatively large SISRE for GLONASS in Sydney and New Zealand are products of large clock errors in satellite R04, which has the equivalent of 45.5cm (1.5ns) of clock errors. If this satellite is discarded the SISRE have a maximum of 10.30 cm. Values that are similar to those of other real-time streams.

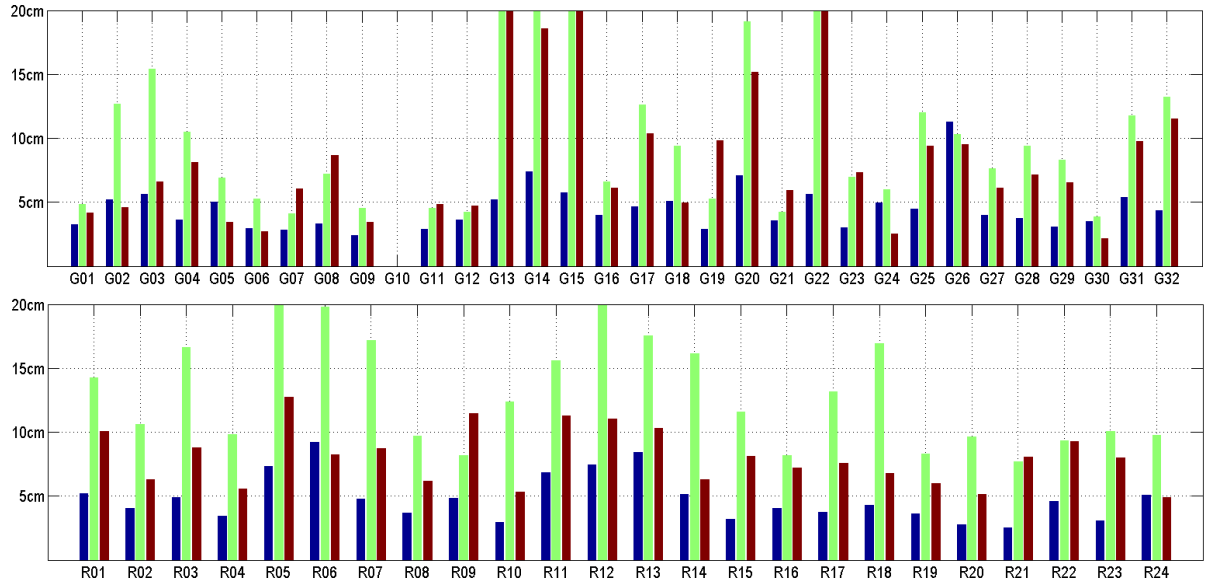

Figure 1. MADOCA orbit errors for GPS (top) and GLONASS (bottom) satellites. Most influential errors are the errors in the Radial directions (blue). Along-track (green) and Cross-track (brown) errors have far less impact on perceived range errors

3.2 Magic GNSS from GMV (CLK81)

Table 4 shows the RMS and daily standard deviation errors for the MagicGNSS generated products. Figure 2 show the RMS errors of orbits calculated by the MagicGNSS software, whereby radial errors are shown in blue, along-track errors are shown in green, cross-track errors are shown in brown. As Figure 2 clearly shows, satellite G26 has very large errors in its calculated orbits and, although not shown in Figure 2, the clock corrections. The orbit, clock errors for this satellite were above 70 cm for all components, and SISRE of up to 1.10 m. These errors significantly affected the PPP performance presented in section 4.

	Radial	**Along**	**Cross**	**Clock**
RMS GPS	9.08 cm	33.53 cm	14.19 cm	19.99 cm
RMS GLO	3.79 cm	9.83 cm	8.73 cm	106.75 cm
STD GPS	5.28 cm	20.23 cm	10.08 cm	13.50 cm
STD GLO	2.24 cm	5.11 cm	4.60 cm	7.41 cm

Table 4. Errors of MagicGNSS satellite orbits and clock estimates, 30th of September 2015.

If the effect of G26 is discarded, daily STD for GPS orbits become 1.67cm for radial, 4.09 cm for along-track and 3.25cm for cross-track errors with clock errors equivalent to 7.77cm. In this case the orbits are significantly better than MADOCA and on par with PPP-Wizard. The clock errors are still slightly larger than those of other systems (driven by a 53cm clock error for G32) however the

over all, SISRE for Sydney and New Zealand are all below 4.52cm, which is better than MADOCA and comparable with PPP-Wizard.

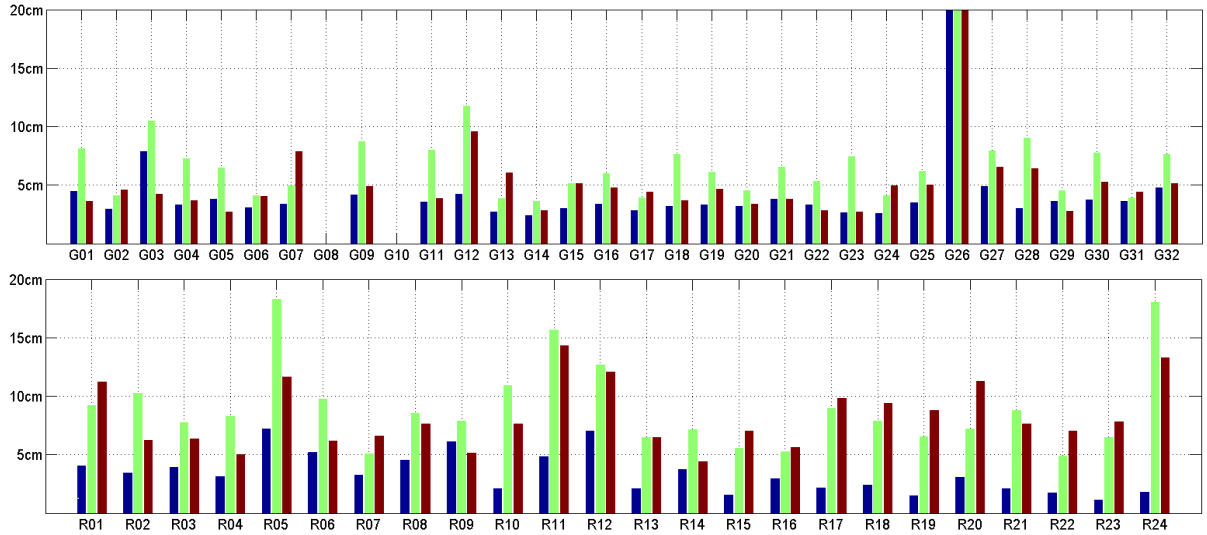

Figure 2. MagicGNSS orbit errors for GPS (top) and GLONASS (bottom) satellites. Errors in Radial, Along-track and Cross-track directions are shown in blue, green and brown. Large errors can be seen for satellite G26.

Unfortunately problems with MagicGNSS's ephemeris for satellite G26 were unknown at the time the PPP solutions in section 4 were calculated, so the errors of satellite G26 affected the PPP solutions. This is also the reason tables 2 and 4 reflect the presence of G26. Had this satellite errors been detected and discarded, performance similar to those of other systems could be expected.

3.3 PPP-Wizard from CNES (CLK9B)

Table 5 shows the RMS and daily standard deviation errors for the PPP-Wizard generated products. Figure 3 shows the RMS errors of orbits. Real-time orbits generated by the PPP-Wizard were the ones closest to the post-processed IGS products for both GPS and GLONASS. This in turn was reflected in SISRE values significantly smaller than the other solutions, below 3.05 cm for GPS.

	Radial	**Along**	**Cross**	**Clock**
RMS GPS	3.11 cm	4.90 cm	4.90 cm	11.03 cm
RMS GLO	2.86 cm	8.32 cm	4.49 cm	55.38 cm
STD GPS	2.24 cm	3.95 cm	3.57 cm	5.19 cm
STD GLO	1.76 cm	4.23 cm	2.40 cm	7.15 cm

Table 5. Errors of PPP-Wizard satellite orbits and clock estimates, 30th of September 2015.

The one exception for this was the 9.41cm SISRE on Bern. Here too, large errors on the G26 satellite orbit and clock estimates influenced the resulting statistic. If satellite G26 is discarded, the SISRE values are all below 3.1 cm.

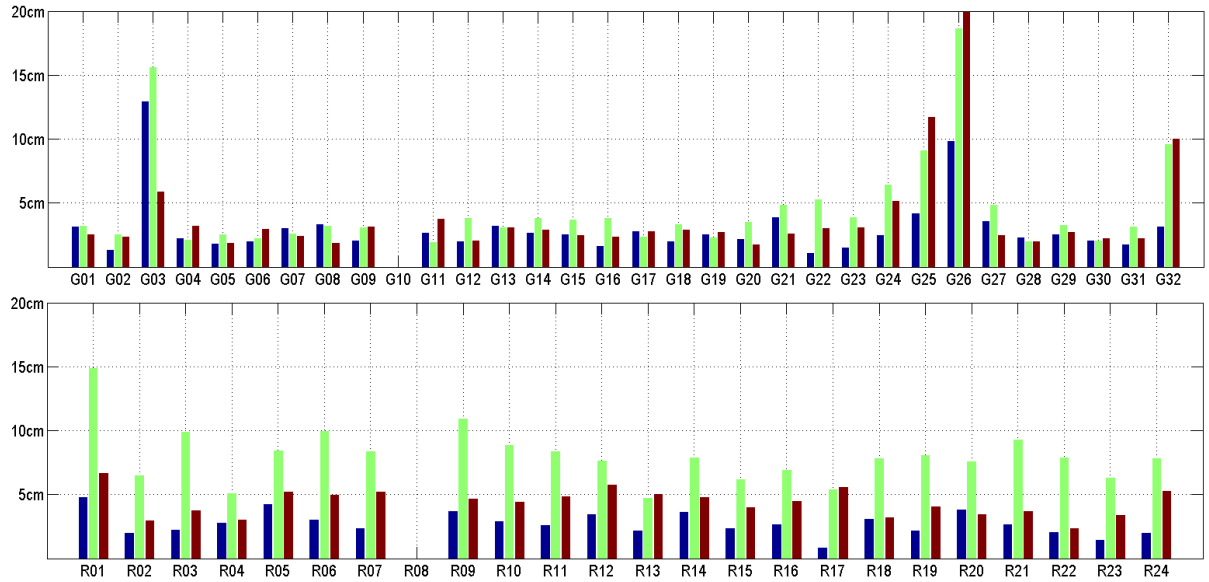

Figure 3. PPP-Wizard orbit errors for GPS (top) and GLONASS (bottom) satellites. Errors in Radial, Along-track and Cross-track directions are shown in blue, green and brown.

It is also to note that the PPP-Wizard stream also transmits phase biases designed to allow PPP with ambiguity resolution and thus lead to precisions on the 2-3 cm level. Although the author have confirmed the benefits of ambiguity resolutions in GPS only solutions (Choy et. al., 2015), ambiguity fixing rates for the test were below 30% in the tests on section 4. It is believed this is because stochastic parameters, specifically the estimated noise of GLONASS observables and ephemeris, were underestimated for the multi-GNSS PPP solutions.

4. PERFORMANCE OF REAL TIME PPP IN NEW ZEALAND

This section present a study of the performance of PPP using the real-time streams explained in section 3. RTCM correction messages were received and decoded in real time. The orbit and clock correction information contained within were combined with the orbit and clocks broadcast by GNSS satellites to obtain precise orbits and clocks.

The precise orbit and clock were used in conjunction with observables taken at various CORS stations to obtain real-time PPP solutions. Figure 4 shows the stations used in the test and their location. PPP-Wizard orbits are based on the IGS-ultra rapid products, which include the stations AUCK, WGTN, DUND, CHTI and a station near the YALD station in Christchurch. MADOCA and MagicGNSS base their products on a network that only includes a station near Dunedin in New Zealand.

This means that the HAST station, which has no nearby station for any network should be able to obtain the same performance as shown here even in cases where local infrastructure are absent. In the same way, MagicGNSS and MADOCA based solutions on AUCK, WGTN YALD or CHTI

should be representative of what potentially can be achieve by satellite based PPP in cases where local infrastructure is unavailable.

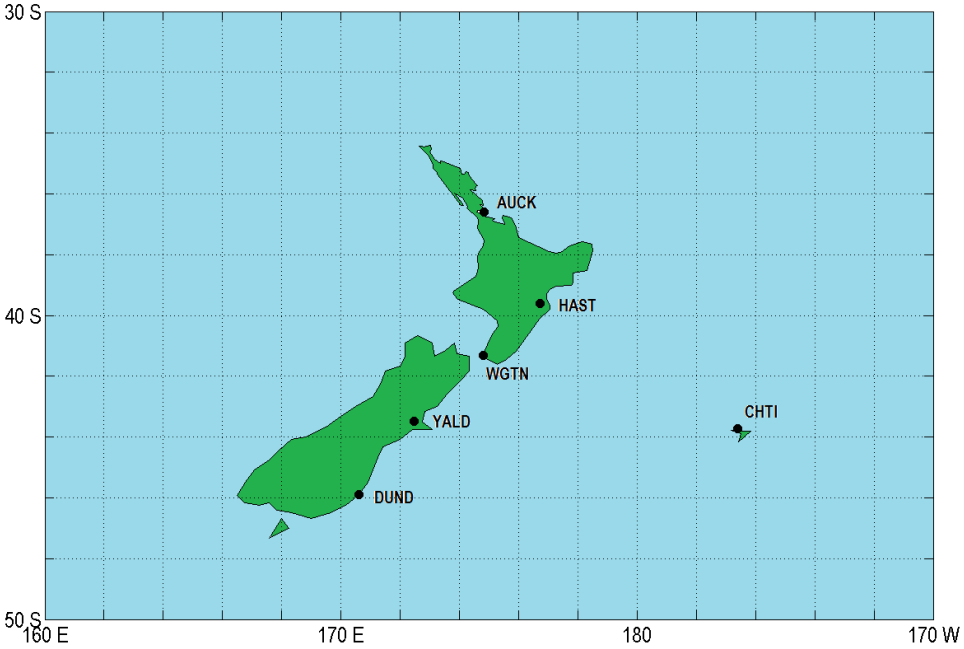

Figure 4. CORS in New Zealand used to calculate PPP Corrections

Real-time solutions were calculated simultaneously for the 6 sites, from the 28th of September to the 3rd of October (except during service outage times). The solutions were restarted after either 6 or 12 hours. A total of 340 solutions were calculated in this way.

Figure 5 shows a sample of real-time PPP solutions calculated on the 1st of October from 18:00 to midnight UTC.

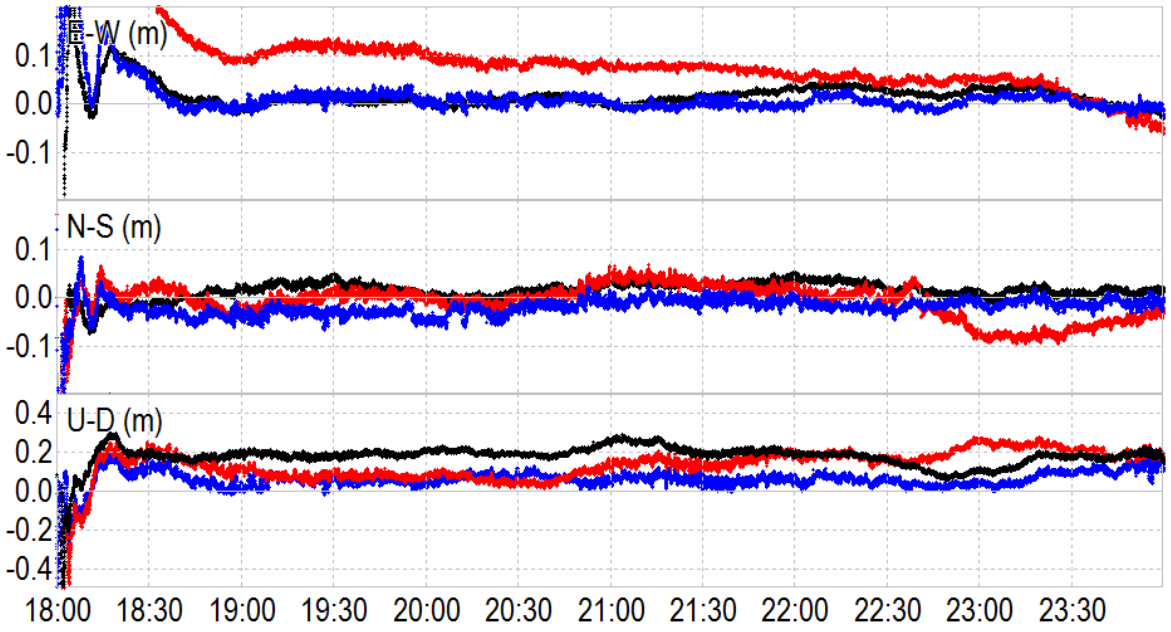

Figure 5. Real-time PPP solutions calculated for the 1st of October 2015. PPP solutions were calculated using MADOCA(black), MagicGNSS (red) and PPP-Wizard (blue) corrections.

The PPP solutions were calculated using observables from the YALD station near Christchurch. The red line represent real-time PPP solutions obtained using MagicGNSS products, the black line represent solutions obtained using MADOCA products, and the blue line represents solutions obtained using PPP-Wizard products. The center of coordinates are ITRF coordinates obtained using Land Information New Zealand's (LINZ) positioning service (LINZ, 2015). The scales in the figure are in meters, with the top graph showing East-West position errors, the middle graph showing North-South errors and the bottom graph showing the Vertical errors a ±0.5m scale (as opposed to the ±0.2 m scale for the horizontal components).

The RMS horizontal accuracy was 4.6 cm for solutions using PPP-Wizard, 6.4 cm for solutions using MADOCA, and 9.7 cm for solutions using MagicGNSS. The RMS vertical accuracy was 8.7 cm for solutions using PPP-Wizard, 10.1 cm for solutions using MADOCA, and 12.7 cm for solutions using MagicGNSS. PPP-Wizard and MADOCA based PPP solutions can be expected to converge to better than 10cm of accuracy within 30 minutes. The RMS of horizontal errors for MagicGNSS based solutions converged to an accuracy better than 10 cm in 127 minutes.

4.1 Positioning Accuracy

Table 6 shows the RMS values for horizontal and vertical errors for real-time PPP solutions obtained using different correction streams in various CORS. The first hour of solutions were discarded in order to give the solutions time to converge and stabilize. An average of 14 to 20 solutions are used to calculate the statistics in table 6.

	Auckland	Chath. Is.	Dunedin	Hastings	Wellington	Yaldhurst
PPP using MDC1	H: 6.13cm V: 10.29cm	H: 5.80cm V: 7.45cm	H: 6.33cm V: 11.35cm	H: 7.43cm V: 9.74cm	H: 6.22cm V: 9.66cm	H: 6.62cm V: 11.46cm
PPP using CLK81	H: 8.71cm V: 12.34cm	H: 10.78cm V: 11.82cm	H: 9.15cm V: 13.53cm	H: 9.86cm V: 12.44cm	H: 9.75cm V: 12.14cm	H: 9.76cm V: 13.61cm
PPP using CLK9B	H: 5.03cm V: 7.69cm	H: 3.39cm V: 8.10cm	H: 4.34cm V: 10.58cm	H: 5.30cm V: 8.10cm	H: 4.98cm V: 7.42cm	H: 4.64cm V: 9.69cm

Table 6. Horizontal and vertical errors of real-time kinematic PPP solutions using real-time corrections from MADOCA (MDC1), Magic GNSS (CLK81) and PPP-Wizard (CLK9B). First 1 hour of measurements were removed in order to allow solutions to converge and stabilize.

The performance of real-time streams are clearly distinguishable, with PPP-Wizard achieving horizontal accuracies better than 5.30 cm for all stations and vertical accuracies of 10.58 cm or better. The accuracies were better than 7.43cm horizontal and 11.46 cm vertical for MADOCA. Finally MagicGNSS give average errors of up to 10.78cm horizontal and 13.61cm vertical. The difference in performance was not significant for different CORS, corroborating the fact that distance from a reference station (used to calculate the PPP corrections) has little influence on the accuracy of the solutions. It is suspected that the MagicGNSS based PPP solutions would have achieved a performance level similar to that of MADOCA if satellite G26 was excluded. PPP algorithms that use currently available real-time PPP products will greatly benefit from algorithms to detect and discard these outliers.

4.2 PPP solution convergence

Figure 6 illustrates the convergence of horizontal positions in real-time PPP solutions using the various correction streams. The red dots represent PPP solutions calculated using MagicGNSS corrections, the blue dots represent solutions using PPP-Wizard corrections and the black dots represent solutions calculated using MADOCA corrections. Figure 7 on the other hand illustrates the convergence of vertical positions in real-time PPP solutions using the various correction streams.

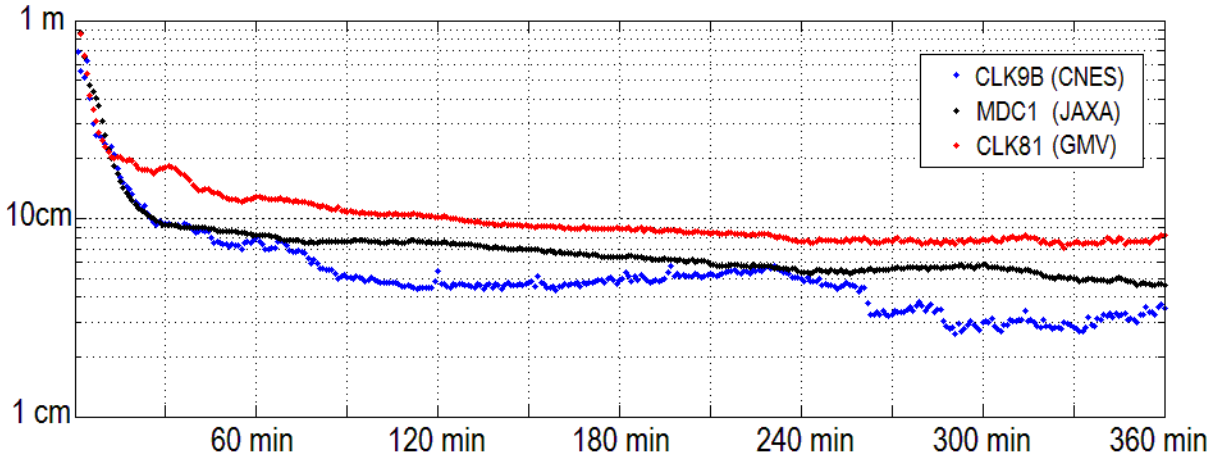

Figure 6. Convergence of horizontal positioning for PPP solutions calculated using MADOCA(black), MagicGNSS (red) and PPP-Wizard (blue) corrections. Values on the figure are the RMS of solutions calculated between 28th of September and 3rd of October 2015. The PPP solutions were calculated using observables from the CORS shown in Figure 4.

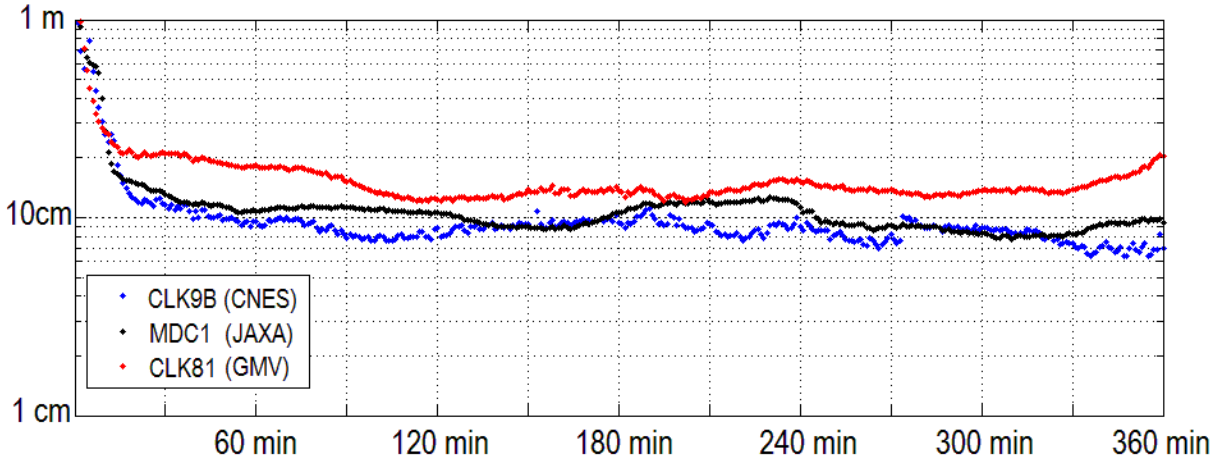

Figure 7. Convergence of vertical positioning for PPP solutions calculated using MADOCA(black), MagicGNSS (red) and PPP-Wizard (blue) corrections. Values on the figure are the RMS of solutions calculated between 28th of September and 3rd of October 2015. The PPP solutions were calculated using observables from the CORS shown in Figure 4.

There are 360 dots of each color in figure 6. Each dot represents the RMS of horizontal errors corresponding to a one minute period (first minute for the first dot, the second minute for the second dot). The RMS is calculated for corresponding samples across all solutions obtained using a particular real-time stream. Figure 7 presents the equivalent statistic for vertical errors.
As it can be seen in figure 6, the solutions using MADOCA and PPP-WIZARD both converge to accuracies better than 10 cm at around the 30 minute mark, specifically 27 minutes for MADOCA and 25 minutes for PPP-Wizard. The MagicGNSS based solutions took 127 minutes to converge below the 10 cm mark.

Vertical accuracies converge below 15 cm of accuracy in 20 minutes for MADOCA and 17 minutes for PPP-Wizard. MagicGNSS converged within 20 cm of the vertical accuracy in 40 minutes. It is to note that although these values have been calculated by averaging more than 100 solutions (and the authors believe this to be representative) convergence time in PPP can vary a lot from solution to solution.

5. SUMMARY

Most of the GNSS based high accuracy positioning services available today are based on differential techniques like RTK. These kinds of services are only available inside a network of Continuously Operating Reference Stations (CORS) or a few kilometers from such stations. An emerging alternative to these infrastructure heavy methods is the Precise Point Positioning (PPP) technique. PPP as a technique that aims to deliver centimeter level accuracy positioning without the need of directly connecting to a local CORS. PPP is well suited for cases where local infrastructure is unavailable or unreliable.

This paper evaluates the three publicly available real-time correction streams for PPP. MADOCA corrections generated by JAXA, MagicGNSS corrections generated by GMV and PPP-Wizard corrections generated by CNES. The Signal in Space Range errors were better than 5 cms for all three products given that some outliers were eliminated. These outliers, particularly satellite G26 for the MagicGNSS were shown to have profound impact in PPP performance. Any practical system to be used in PPP must be equipped with monitoring systems to detect and discard these outliers.

Horizontal accuracy of real-time PPP was found to be 4.6 cm for solutions using PPP-Wizard, 6.4 cm for solutions using MADOCA, and 9.7 cm for solutions using MagicGNSS. Vertical accuracies were 8.7 cm for solutions using PPP-Wizard, 10.1 cm for solutions using MADOCA, and 12.7 cm for solutions using MagicGNSS. The MagicGNSS solutions are expected to have better performance as long as outliers like G26 in this can be detected and discarded. MADOCA and PPP-Wizard can be expected to converge within 10 cm of horizontal accuracy and 15 cm vertical accuracy within 30 minutes.

Although the accuracies and convergence time are not yet at the level of commercial RTK services, PPP based solutions are much more flexible and cost effective to deploy. With the use of satellite delivery, which is under study or development by multiple agencies around the world, these type of services could become available anywhere in the world, independent of the availability of local infrastructure.

ACKNOWLEDGEMENTS
This research is funded through the Australian Cooperative Research Centre for Spatial Information (CRCSI Project 1.11) and is a collaborative project between the CRCSI and the Japan Aerospace Exploration Agency (JAXA). The CRCSI research consortium consists of RMIT University, University of New South Wales, Victoria Department of Environment and Primary Industry, New South Wales Land and Property Information and Geoscience Australia. The authors would also like to thank JAXA for maintaining the MDC1 real-time streams, the CNES for maintaining the CLK9B real-time and IGS for allowing access to the CLK81 stream.

REFERENCES

Chang, X. W., Yang X., Zhou T. (2009), "MLAMBDA: a modified LAMBDA method for integer least-squares estimation", Journal of Geodesy, Vol. 79, No 9, 2005, p 552-565

Ge M., Gendt G., Rothacher M., Shi C., Lui J., (2007), "Resolution of GPS carrier-phase ambiguities in Precise Point Positioning (PPP) with daily observations," Journal of Geodesy, vol. 82, pp. 389–399, 2007.

GMV (2015), MagicGNSS Brochure, http://magicgnss.gmv.com/magicGNSS_brochure.pdf Accessed August 2015.

Grinter, T., Jansen V., (2012). "Post-Processed Precise Point Positioning: A Viable Alternative?", Proceedings of the 17th Association of Public Authority Surveyors Conference (APAS2012), Wollongong, New South Wales, Australia, 19-21 March 2012.

Harima K., Choy S., Li Y., Choudhury M., Rizos C., and Kogure S. 2015, "Pilot Study on the use of Quasi-Zenith Satellite System as a GNSS Augmentation System for High Precision Positioning in Australia", Proceeding of the IGNSS Symposium, July 2015, Gold Coast, Australia, Paper 27

IGS, (2015). "Real-time Service", http://rts.igs.org/, Accessed September 2015.

IGS, (2014). "International GNSS Service",http://igscb.jpl.nasa.gov/, Accessed January 2014.

JAXA, (2014), "Interface Specification for QZSS (version 1.6)". http://qz-vision.jaxa.jp/USE/is-qzss/DOCS/IS-QZSS_15D_E.pdf, November 2014

Kouba, J., (2009), "A Guide to using International GNSS Service (IGS) Products", http://igscb.jpl.nasa.gov/components/usage.html, Accessed October 2009.

Laurichesse D., Mercier F., Berthias J., Broca P., Cerri L., (2009), "Integer Ambiguity Resolution on Undifferenced GPS Phase Measurements and Its Application to PPP and Satellite Precise Orbit

Determination," NAVIGATION: Journal of The Institute of Navigation, vol. 56, pp. 135 - 149, 2009.

LINZ, (2015). “Land Information New Zealand’s PositioNZ service”, http://www.linz.govt.nz/data/geodetic-services/positionz, Accessed December 2015.

RTCM (2013), "RTCM STANDARD 10403.2 for differential GNSS," in RTCM 10403.2, ed. Arlington, Virginia: Radio Technical Commision for Maritime Services, 2013.

Takasu T. and Yasuda A. (2009): “Development of the low-cost RTK-GPS receiver with an open source program package RTKLIB”, International Symposium on GPS/GNSS, Jeju, Korea, November 2009.

Zumberge, J. F., Heflin M. B., Jefferson D.C., Watkins M. M. Webb F. H., (1997). “Precise Point Positioning for The Efficient and Robust Analysis of GPS Data From Large Networks”, Journal of Geophysical Research, 102, B3, 5005-17.

BIOGRAPHICAL NOTES

Ken Harima obtained his Bachelor’s degree in Elctronic Engineering from Universidad Simon Bolivar, Caracas Venezuela, in 2002. He obtained PhD degree from the University of Tokyo in 2012.He is currently a research fellow at the School of Mathematical and Geospatial Sciences in RMIT University. He research interest are GNSS augmentation and SBAS systems.

Suelynn Choy completed her PhD in 2009 in the area of GPS Precise Point Positioning (PPP) at RMIT University, Australia. Since then, she works as a full-time academic staff at the School of Mathematical and Geospatial Sciences in RMIT University. She teaches land surveying, geodesy, and GNSS navigation to undergraduate and graduate students. Her current research interests are in the areas of multi-GNSS PPP and using GNSS for atmospheric and ground remote sensing. Suelynn is the co-chair of the IAG (International Association of Geodesy) Working Group 4.5.2: PPP and Network RTK under Sub-Commission 4.5: High Precision GNSS Algorithms and Applications.

Chris Rizos is a graduate of the School of Surveying, The University of New South Wales(UNSW), Sydney, Australia; obtaining a Bachelor of Surveying in 1975, and a Doctor of Philosophy in 1980 in Satellite Geodesy. He is currently a member of the School of Civil & Environmental Engineering, UNSW. Chris research experitise is high precision applications of GPS. He is a member of a Fellow of the Australian Institute of Navigation, a Fellow of the U.S. Institute of Navigation, a Fellow of the International Association of Geodesy (IAG), an honorary professor of Wuhan University (P.R. China), and is currently President of the IAG (2011-2015).

Satoshi Kogure is Mission Manager for QZSS operation and technical demonstration in Satellite Navigation Office, Japan Aerospace Exploration Agency (JAXA). He received an MS in aeronautical engineering from Nagoya University in 1993 and an MS in aerospace engineering from University of Colorado at Boulder in 2001. He has been working for the development of Japanese satellite positioning system, QZSS as a satellite systems engineer since 2001. He is a member of Japan Society for Aeronautical and Space Science, Institute of Positioning, Navigation and Timing of Japan as well as U.S. Institute of Navigation.

CONTACTS

Dr. Ken Harima.
Royal Melbourne Institute of Technology (RMIT) University
GPO Box 2476V, Melbourne, Victoria 3001, Australia
Tel: +61 3 9925 3775
Email: ken.harima@rmit.edu.au

Dr. Suelynn Choy
Royal Melbourne Institute of Technology (RMIT) University
GPO Box 2476V, Melbourne, Victoria 3001, Australia.
Tel: +61 3 9925 2650
Fax: +61 3 9663 2517
Email: suelynn.choy@rmit.edu.au

Dr. Chris Rizos
The University of New South Wales
UNSW Sydney NSW 2052 AUSTRALIA
Tel: +61 2 93854205
Fax: +61 2 9385 6139
Email: c.rizos@unsw.edu.au

Mr. Satoshi Kogure
Japan Aerospace Exploration Agency
Tsukuba Space Center, 2-1-1 Sengen, Tsukuba, Ibaraki, Japan
Tel : +81 50 3362-3558
Fax : +81 29 868-5987
Email: kogure.satoshi@jaxa.jp